

Coulomb excitation of $^{112, 116}\text{Sn}$

H.J. Wollersheim, P. Doornenbal, J. Gerl

(Gesellschaft für Schwerionenforschung, P.O.Box 110552, D-64291 Darmstadt, Germany)

R.K. Bhowmik, S. Muralithar, R.P. Singh, R. Kumar, A. Jhingan

(Inter University Accelerator Centre, P.O.Box 10502, New Delhi 110067, India)

S.K. Mandal

(Department of Physics and Astrophysics, University of Delhi, Delhi 110007, India)

Abstract

It is proposed to measure the $B(E2, 0^+ \rightarrow 2^+)$ values of the first excited state in $^{112, 116}\text{Sn}$ with Coulomb excitation using a ^{58}Ni beam at an energy of 190 MeV. The gamma-rays from the de-excitation will be measured with the local Ge-array. Information of the scattering angle, needed for a good Doppler-shift correction and impact parameter selection will be extracted from an annular position sensitive parallel plate avalanche counter (PPAC). The experimental results are of great interest for the comparison with sophisticated shell model calculations.

1 Physics motivation

The $B(E2)$ values of shell model calculations for the even tin isotopes $^{102-130}\text{Sn}$ show a parabola-like trend, as can be seen in figure 1, which resembles the typical behaviour of a one-body even tensor operator across a shell in the seniority scheme[1]. Thus, for a seniority changing transition, the $B(E2)$ values increase at first, then flatten, peak at mid-shell and fall off thereafter.

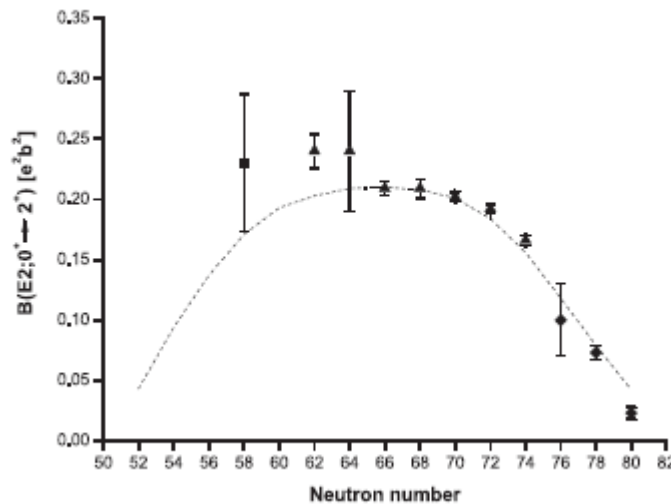


Figure 1: Comparison of experimental $B(E2)$ values of Sn isotopes with the theoretical predictions (dotted curve). Picture taken from [2]

Existing experimental data show an almost perfect agreement with this plot for tin isotopes heavier than $A = 114$ [3][4], hence only if at least half of the major shell $N = 50 - 82$ is filled. In the case of lighter stable tin isotopes, which have a natural abundance of less than 1%, the publications for ^{112}Sn [5][6][7] and ^{114}Sn [8][9][10] yield higher $B(E2)$ values than expected, but so far big experimental errors prohibit further theoretical interpretations. One main reason for these errors is that these experiments either have used enriched targets, then

the uncertainty stems from the impurity of the target, or used the recoil distance Doppler-shift (RDDS) method which is error prone for lifetimes lower than 1ps.

In 2006, two Coulomb excitation experiments were performed successfully at GSI which used $^{114,116}\text{Sn}$ projectiles and a ^{58}Ni target. The extracted reduced transition probabilities will be published soon.

The B(E2) value obtained for the unstable ^{108}Sn [2] in a RISING experiment is based on a relative B(E2) measurement to ^{112}Sn . Since the present error in ^{112}Sn is significant, a more precise measurement of ^{112}Sn would also decrease the error of ^{108}Sn .

The aim of this experiment is hence to study the detailed structure of very rare stable ^{112}Sn isotope with an error of less than 3% (FWHM) for the B(E2) value, while ^{116}Sn serves as calibration point.

2 Experimental details

The proposed Coulomb excitation experiment will be performed at the IUAC accelerator using a ^{58}Ni beam of 190 MeV and highly enriched $1\text{mg}/\text{cm}^2$ Sn targets (enrichment >99.5%). Since it is planned to make a double relative B(E2) measurement, which means the normalized intensity ratios of ^{58}Ni projectile excitation to the Sn target excitation will be compared with the calibration run, good statistics are needed in all projectile and target excitation cases. Therefore, we aim for peak integrals of 10^4 counts per $2^+ \rightarrow 0^+$ transition.

The gamma decays will be measured with four clover Ge-detectors. We intend to have a resolution of better than 1%. Assuming an intrinsic resolution of these detectors of 0.3% and a β of 0.05, the distance of the Ge-detectors to the target will be put to 15 cm, which results in a photo peak efficiency of 3% at 1.3 MeV.

The scattering angles of the heavy ions will be measured with a position sensitive annular parallel plate avalanche counter (PPAC), which covers scattering angles of $\theta_{\text{lab}} = 15^\circ - 45^\circ$ and $\phi_{\text{lab}} = 0 - 360^\circ$. Because the projectiles as well as the target nuclei will be detected in the PPAC (however not simultaneously), the opening angle of the PPAC corresponds to an angular coverage of $23^\circ \leq \theta_{\text{cm}} \leq 67^\circ$ and $90^\circ \leq \theta_{\text{cm}} \leq 150^\circ$ in the center of mass system, respectively. The excitation of the 2^+ state at 1.257 MeV is clearly separated for both impact parameter regions and will also not be disturbed by the target excitation (2^+ state at 1.454 MeV). For both impact parameter regions a cross section of 120mb is estimated.

Including the setup of the electronics and the calibration runs we ask for 3 days of beam time which assumes a beam current of 1pA.

References

- [1] R. Casten, Nucl. Structure from a Simple Perspective. Oxford University Press Inc., N New York (2000).
- [2] A. Banu, PhD. Thesis, 2005
- [3] S. Raman, Atomic Data and Nuclear Data Tables 78, 1-129 (2001)
- [4] D.C. Radford et al., Nucl. Phys. A 746, 83c-89c (2004)
- [5] Atomic Data and Nuclear Data Tables, Volume 36, Issue 1, 1987, 1-96
- [6] R. Greatzer et al., Phys. Rev. C 12, 1462-1468 (1975)
- [7] P.H. Stelson et al., Phys. Rev. C2, 2015-2022 (1970)
- [8] D.S. Andreev et al., Izvest. Akad. Nauk SSSR, Ser.Fiz 25, 832 (1961)

- [9] J. Gableske et al., Nucl. Phys. A, Vol. 691, (2001) 551-576
 [10] I.N. Vishnevsky et al., Proc. 41st Ann. Conf. Nucl. Spectrosc. Struct. At. Nuclei, Minsk, p. 71 (1991)

Appendix A: Kinematics $^{112}\text{Sn} + ^{32}\text{S}$ at 105 MeV

$\theta_{\text{cm}}(\text{degree})$	$\Psi_{\text{lab}}(\text{degree})$	$E_3(\text{MeV})$	$E_4(\text{MeV})$	$\zeta_{\text{lab}}(\text{degree})$
10	7.8	104.4	0.6	85
20	15.6	102.8	2.2	80
30	23.5	100.1	4.9	75
40	31.4	96.5	8.5	70
50	39.5	92.0	13.0	65
60	47.8	86.9	18.1	60
70	56.3	81.1	23.9	55
80	65.0	75.0	30.0	50
90	74.1	68.7	36.3	45
100	83.5	62.4	42.6	40
110	93.4	56.3	48.7	35
120	103.9	50.6	54.4	30
130	115.0	45.4	59.6	25
140	126.8	40.9	64.1	20
150	139.3	37.3	67.7	15
160	152.4	34.6	70.4	10
170	166.1	33.0	72.0	5

Appendix B: Kinematics $^{112}\text{Sn} + ^{58}\text{Ni}$ at 190 MeV

$\theta_{\text{cm}}(\text{degree})$	$\Psi_{\text{lab}}(\text{degree})$	$E_3(\text{MeV})$	$E_4(\text{MeV})$	$\zeta_{\text{lab}}(\text{degree})$
10	6.6	188.7	1.3	85
20	13.2	184.8	5.2	80
30	19.9	178.6	11.4	75
40	26.6	170.0	20.0	70
50	33.4	159.5	30.5	65
60	40.4	147.3	42.7	60
70	47.5	133.8	56.2	55
80	54.9	119.4	70.6	50
90	62.6	104.6	85.4	45
100	70.7	89.8	100.2	40
110	79.4	75.4	114.6	35
120	88.8	61.9	128.1	30
130	99.3	49.7	140.3	25
140	111.1	39.2	150.8	20

150	124.9	30.6	159.4	15
160	141.0	24.3	165.7	10
170	159.6	20.5	169.5	5

Appendix C: Coulomb excitation $^{112}\text{Sn} + ^{32}\text{S}$ at 105 MeV

$\theta_{\text{cm}}(\text{degree})$	$d\sigma/d\Omega$ (b/sr)	$d\sigma/d\Omega * \sin(\theta_{\text{cm}})$
10	$0.0093*10^{-2}$	$0.0016*10^{-2}$
20	$0.6594*10^{-2}$	$0.2255*10^{-2}$
30	$1.749*10^{-2}$	$0.8745*10^{-2}$
40	$2.336*10^{-2}$	$1.502*10^{-2}$
50	$2.474*10^{-2}$	$1.895*10^{-2}$
60	$2.379*10^{-2}$	$2.060*10^{-2}$
70	$2.191*10^{-2}$	$2.059*10^{-2}$
80	$1.973*10^{-2}$	$1.943*10^{-2}$
90	$1.761*10^{-2}$	$1.761*10^{-2}$
100	$1.568*10^{-2}$	$1.544*10^{-2}$
110	$1.400*10^{-2}$	$1.316*10^{-2}$
120	$1.257*10^{-2}$	$1.089*10^{-2}$
130	$1.140*10^{-2}$	$0.8733*10^{-2}$
140	$1.046*10^{-2}$	$0.6724*10^{-2}$
150	$0.9741*10^{-2}$	$0.4871*10^{-2}$
160	$0.9239*10^{-2}$	$0.3160*10^{-2}$
170	$0.8942*10^{-2}$	$0.1553*10^{-2}$

Ψ_{lab} (degree)	θ_{cm} (degree)
15	19.2
45	56.7

$$\int_{-\pi}^{\pi} \int_{19.2^{\circ}}^{56.7^{\circ}} \frac{d\sigma}{d\Omega} \sin \theta d\theta d\phi = 52[\text{mb}] \quad \int_{-\pi}^{\pi} \int_{90^{\circ}}^{150^{\circ}} \frac{d\sigma}{d\Omega} \sin \theta d\theta d\phi = 73[\text{mb}]$$

Appendix D: Coulomb excitation $^{112}\text{Sn} + ^{58}\text{Ni}$ at 190 MeV

$\theta_{\text{cm}}(\text{degree})$	$d\sigma/d\Omega$ (b/sr)	$d\sigma/d\Omega * \sin(\theta_{\text{cm}})$
10	$0.0004*10^{-1}$	$0.0001*10^{-1}$
20	$0.0735*10^{-1}$	$0.0251*10^{-1}$
30	$0.2500*10^{-1}$	$0.1250*10^{-1}$
40	$0.3705*10^{-1}$	$0.2382*10^{-1}$
50	$0.4149*10^{-1}$	$0.3178*10^{-1}$
60	$0.4098*10^{-1}$	$0.3549*10^{-1}$
70	$0.3813*10^{-1}$	$0.3583*10^{-1}$
80	$0.3439*10^{-1}$	$0.3387*10^{-1}$
90	$0.3051*10^{-1}$	$0.3051*10^{-1}$
100	$0.2687*10^{-1}$	$0.2646*10^{-1}$
110	$0.2363*10^{-1}$	$0.2221*10^{-1}$
120	$0.2086*10^{-1}$	$0.1807*10^{-1}$
130	$0.1856*10^{-1}$	$0.1422*10^{-1}$
140	$0.1672*10^{-1}$	$0.1075*10^{-1}$

150	$0.1532 \cdot 10^{-1}$	$0.0766 \cdot 10^{-1}$
160	$0.1435 \cdot 10^{-1}$	$0.0491 \cdot 10^{-1}$
170	$0.1376 \cdot 10^{-1}$	$0.0239 \cdot 10^{-1}$

Ψ_{lab} (degree)	θ_{cm} (degree)
15	22.7
45	66.5

$$\int_{-\pi 22.7^0}^{\pi 66.5^0} \frac{d\sigma}{d\Omega} \sin \theta d\theta d\phi = 120 [mb] \quad \int_{-\pi 90^0}^{\pi 150^0} \frac{d\sigma}{d\Omega} \sin \theta d\theta d\phi = 122 [mb]$$